

Cement and Concrete Research

Effect of alkalinity on early age hydration in calcium sulfoaluminate clinker

--Manuscript Draft--

Manuscript Number:	CEMCON-D-21-01461
Article Type:	Research paper
Keywords:	calcium sulfoaluminate clinker, early hydrations, alkalis, continuous and discontinuous DRX.
Abstract:	<p>The early hydrations of calcium sulfoaluminate clinker (CSA) in neutral or alkaline solutions (0 M, 0.1 M, 1 M, 4 M and 8 M NaOH) was studied by isothermal conduction calorimetry, X-ray diffraction (both continuous and discontinuous (after isopropanol hydration stopped), and infrared spectroscopy. With 0.1 M, a similar behavior to water hydration was obtained. However, with 1 M, a delay in the reaction rate is observed mainly associated with the lower stability of AFt in the 1 M NaOH solution. Faster hydration but lower total heat was obtained in the KCSA-2M pastes, associated with the formation of different reaction products (a metastable U phase that becomes AFt, C_3AH_6 and tenardite). Hydration with very alkaline (4M and 8M) solutions inhibited AFt formation completely, although ye'elimite reacted more vigorously (particularly with 8 M NaOH) to form katoite, AH_3 and thenardite.</p>

Highlights

- Effect of alkalinity in the early hydration of a calcium sulfoaluminate clinker (KCSA)
- Isothermal conduction calorimetry correlation with continuous and discontinuous XRD
- The initial reaction of KCSA with 1 M, 2 M or 4 M NaOH is slower than with water
- The initial reaction of KCSA with 8M NaOH is faster but AFt is not formed

Effect of alkalinity on early age hydration in calcium sulfoaluminate clinker

P. Padilla-Encinas^a, L. Fernández-Carrasco^b, A. Palomo^a, A. Fernández-Jiménez^{a*}

^aInstituto de Ciencias de la Construcción Eduardo Torroja, (IETcc-CSIC), Departamento de materiales, Madrid, Spain

^bAnálisis y Tecnología de Estructuras y Materiales (ATEM), Departament de Enginyeria Civil i Ambiental, Universitat Politècnica de Catalunya – Barcelona TECH

*Corresponding author. *E-mail address:* anafj@ietcc.csic.es (A. Fernandez-Jimenez).

Abstract

The early hydrations of calcium sulfoaluminate clinker (CSA) in neutral or alkaline solutions (0 M, 0.1 M, 1 M, 4 M and 8 M NaOH) was studied by isothermal conduction calorimetry, X-ray diffraction (both continuous and discontinuous (after isopropanol hydration stopped), and infrared spectroscopy. With 0.1 M, a similar behavior to water hydration was obtained. However, with 1 M, a delay in the reaction rate is observed mainly associated with the lower stability of AFt in the 1 M NaOH solution. Faster hydration but lower total heat was obtained in the KCSA-2M pastes, associated with the formation of different reaction products (a metastable U phase that becomes AFt, C₃AH₆ and tenardite). Hydration with very alkaline (4M and 8M) solutions inhibited AFt formation completely, although ye'elimite reacted more vigorously (particularly with 8 M NaOH) to form katoite, AH₃ and thenardite.

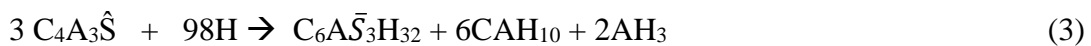
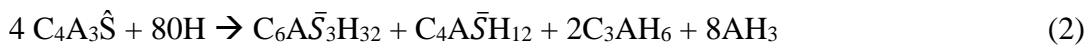
Keywords: calcium sulfoaluminate clinker, early hydrations, alkalis, continuous and discontinuous DRX.

1 Introduction

The main component of calcium sulfoaluminate cement (CSA) is ye'elimite, for which Fukuda assigned the chemical composition $C_4A_3\hat{S}$ [1]. Interest in CSA [1-5] has been growing of late, for its manufacture emits less CO_2 and its clinkerisation calls for lower temperatures than the major phase in portland cement (PC). The CO_2 emissions associated with $C_4A_3\hat{S}$ are on the order of 0.22 kg/mol vs the 0.58 kg/mol emitted by C_3S and the enthalpy involved in $C_4A_3\hat{S}$ formation is 800 kJ/kg compared to 1848 kJ/kg in C_3S [6-7].

As CSA cement is manufactured in rotary kilns with raw materials containing more alumina and sulfate than portland cement, it is synthesised from limestone, bauxite or aluminous clay [1-5]. At 1300 °C, sintering temperatures are substantially lower than required for portland cement. CSA cement began to be manufactured on an industrial scale in the nineteen seventies, primarily in China. The Chinese Academy of Construction Materials determined that the optimal composition was ye'elimite ($C_4A_3\hat{S}$), belite (C_2S), ferrite and anhydrite ($CaSO_4$) [4], along with minority phases such as C_4AF , $C_{12}A_7$, C_3A , C_6AF_2 , C_2SH_8 and periclase [1-4]. CSA cements vary in their composition, however, and depending on the raw materials used may also contain ternesite ($C_5S_2\hat{S}$) [3]. As CSA clinker may have a fairly low (16 % to 25 %) calcium sulfate content, preferably in the form of gypsum, may be added during grinding to enhance setting and favour ettringite formation [4-5].

CSA cements are characterised by the development of high early-age mechanical strength and short setting times, both associated with the early-age formation of abundant ettringite. Ye'elimite hydration in the absence of calcium sulfate, depending on the amount of water present, is described in Equations 1 and 2. With 'normal' amounts of water, monosulfoaluminate and aluminium hydroxide form. In the presence of excess water, the products are ettringite ($C_6A_3\hat{S}H_{32}$) and calcium aluminate hydrates (Equations 1-3) [1-5].



Depending on ettringite formation rate and microstructure, calcium sulfoaluminate cements may be used as shrinkage-resistant, self-stressing or high early-age strength cements [8-11].

The presence of alkalis at certain concentrations has been observed to have a substantial effect on ye'elimite hydration. Winnefeld et al. [2] reported that when ye'elimite was hydrated with 0.01 M to 0.1 M potassium hydroxide, reaction kinetics rose with medium pH. Ogawa et al. [12] obtained similar results, with the ye'elimite hydration rate rising at NaOH concentrations of 0.05 M to 2.0 M. At very high NaOH concentrations (~8 M) and high pH, however, ettringite has been found to be unstable, forming hydrogranate, thenardite and nordstrandite.

Zhang et al. [13] studied the effect of 0 M, 0.01 M, 0.1 M, 1 M, 5 M and 8 M NaOH on the microstructure of the alumina trihydrate forming with CSA hydration. They observed the degree of AH_3 crystallinity to depend on pH, exhibiting nano-crystallinity at low concentrations but full crystallinity at high NaOH content. Studying commercial CSA hydration at NaOH concentrations of 0 M, 0.1 M, 1 M, 4 M and 8 M, Tambara et al. [14] found that at low concentrations the products were AFt and amorphous AH_3 , whereas at high concentration U-phase, thenardite and monocrystalline AH_3 formed. The authors of the present paper also recently published an article on the effect of alkalis on later age hydration of CSA clinker (KCSA) [15]. In that study low NaOH concentrations (0 M, 0.1 M, 1 M and 2 M) were found to induce the formation of ettringite and AH_3 , whereas at high concentrations (4 M and 8 M) the products obtained were thenardite and katoite. One of the conclusions drawn was the need for a detailed study of very early age hydration, which is when these processes are most intense.

This study is, then, an extension of the research reported in the aforementioned article [15]. It aims to fill some of the knowledge gaps around the effect of alkali content on early KCSA hydration. It therefore compares normal water-based hydration to hydration in the presence of Na^+ and OH^- concentrations of 0.1 M to 8 M. At this point, it should be noted that this study forms part of a broader work where the effect of alkalis on hydration of both a CSA cement and clinker (KCSA) is studied in order to make blended [16-17] and hybrid [18-20] cements. In hybrid cements, alkalis are incorporated to accelerate the reaction of the supplementary cementitious materials (SCMs) [16-20].

2. Experimental

2.1. Materials

The i.tech ALI PRE GREEN industrial calcium sulfoaluminate clinker (KCSA) used in this study was supplied by HeidelbergCement Hispania. KCSA chemical composition was

determined with X-ray fluorescence and its mineralogy with X-ray diffraction (Table 1). Rietveld analysis of the phases identified was conducted with TOPAS software.

Table 1. KCSA chemical and mineralogical composition

Chemical composition (%)	Mineralogical composition ² (%)
CaO = 40.82	Ye'elimite = 68.4±0.99
SiO ₂ = 9.51	Bredigite = 7.40±0.37
Al ₂ O ₃ = 29.37	Belite = 16.90±1.03
Fe ₂ O ₃ = 1.32	Periclase = 3.67±0.21
MgO = 4.13	Gehlenite = 1.90 ±0.44
Na ₂ O = 1.06	C ₃ A = 1.75±0.39
K ₂ O = 0.47	
TiO ₂ = 0.39	
SO ₃ = 9.92	
Other = 1.70	
LoI ¹ = 1.31	
Blaine fineness (cm ² /g) = 4088.2	

¹Loss on ignition; ²International Centre for Diffraction Data; ICDD² No.: ye'elimite (Y): 33-0256; bredigite (B): 36-399; belite (b): 86-0398; periclase (P): 4-829; gehlenite (g): 35-755; C₃A: 38-1429.

2.2. Analytical tools and methodology

The KCSA pastes were hydrated at a liquid/cement ratio of 0.5 with distilled, deionised water bearing 0 M, 0.1 M, 1 M, 2 M, 4 M or 8 M NaOH. Heat release at 25°C, was determined with isothermal conduction calorimetry on a TAM Air system. After 10 g of clinker were stirred for 3 min in 5 g of liquid, 7.5 g of the solution were placed in the calorimeter, using distilled water (3.45 g) as the internal standard.

Continuous (in-situ) X-ray diffraction was conducted at times selected in keeping with heat flow curves on a BRUKER D8 ADVANCE analyser fitted with: a 3 kW high voltage generator, a copper anode X-ray tube (K α 1, 2, 1.540 Å Cu radiation; standard 40 kV, 50 mA operation) and a non-monochromatic (=K α 2) Lynxeye detector bearing a 3 mm anti-scatter slit and a 0.5 % Ni K β filter. The cement was mechanically stirred into the respective liquid medium for 3 min and placed in a Kapton film-lidded sample holder. Readings were taken at 30 min intervals across a 2 θ range of 5° to 45° at a step size of 0.01973° and a step time of 0.9 s.

Discontinuous XRD analyses were also conducted on samples in which the hydration reactions were detained at times determined on the grounds of the calorimetric curves by immersing the crushed pastes in isopropanol. The suspensions were subsequently filtered and vacuum-dried for 3 d prior to analysis. The resulting powder samples were X-ray

112 diffracted on the same diffractometer as described for continuous XRD using a 6 mm
113 variable divergence slit at a 2θ range of 5° to 60° , a 0.5 s step time and a 0.02° step size.

114 Fourier transform infrared spectroscopy analysis was conducted on an ATI Mattson Genesis
115 spectrophotometer. Pellets consisting in 1.0 mg of dry KCSA cement samples prepared as
116 for XRD and pressed into 200 mg pellets of KBr were scanned in the 4000 cm^{-1} to 400 cm^{-1}
117 range at a spectral resolution of 4 cm^{-1} . The wavelength accuracy at each data point was
118 better than 0.01 cm^{-1} .

120 3 Results

121 3.1 Calorimetric curves

122 [Figure 1](#) depicts the heat released by all the pastes in the first 200 h, during which all the
123 curves plateaued, denoting a high degree of reaction. Exceptionally, in the paste hydrated at
124 4 M the reaction was extended for up to 1200 h to ensure stabilisation. The KCSA pastes
125 hydrated with water, 0.1 M or 1 M exhibited very similar 200 h total heat values
126 ($\sim 386/378/373\text{ J/mol}$), although the respective peak was retarded in the 1 M material. At
127 2 M, $\sim 320\text{ J/mol}$ were released after 200 h. At 4 M the value was initially lower, but heat
128 release was similar ($\sim 314\text{ J/mol}$) when the curve ultimately plateaued at 1200 h. In contrast,
129 at 8 M less total heat was released ($\sim 180\text{ J/mol}$), whilst the plateau was reached at $\sim 50\text{ h}$,
130 denoting a higher reaction rate than in the other pastes. Portland cement with greater heat of
131 hydration is normally associated with a higher degree of reaction [\[10,16,21\]](#). As discussed
132 later, here that was not necessarily the case, however, for reactivity was also observed to
133 depend on the nature of the hydration products formed, in turn was impacted by medium
134 alkalinity.

135 The heat flow curve ([Figure 2](#)) generated when KCSA was hydrated with water (KCSA-H)
136 exhibited a signal in the first 30 min of the reaction associated with initial KCSA dissolution.
137 It was followed at around 1.4 h by a second, which preceded the induction period. After 5 h
138 two other signals were observed, peaking at round 6.5 h and 11 h. The curve for the KCSA
139 sample hydrated with 0.1 M NaOH (KCSA-0.1 M) exhibited only minor differences to the
140 one observed for the water-hydrated paste, although all the signals were less intense and
141 appeared at older ages (the second at around 6.6 h, the third, a shoulder, at around 11.8 h and
142 the fourth at around 18 h). The signals on the KCSA-1M curve included one at 30 min,

associated with the reaction between KCSA and the 1 M NaOH, followed by a low intensity shoulder at 3.6 h. That in turn preceded an induction period longer than observed for the water-hydrated paste, culminating in a peak at around 107 h.

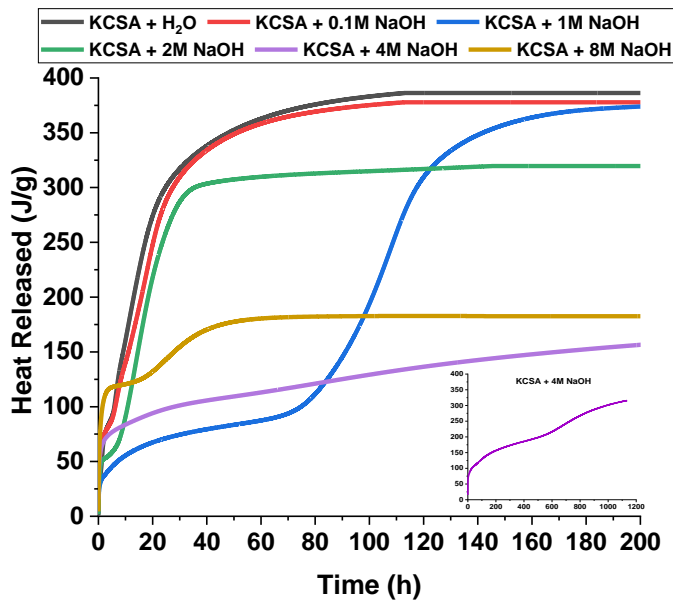


Figure 1. Total heat of hydration curves

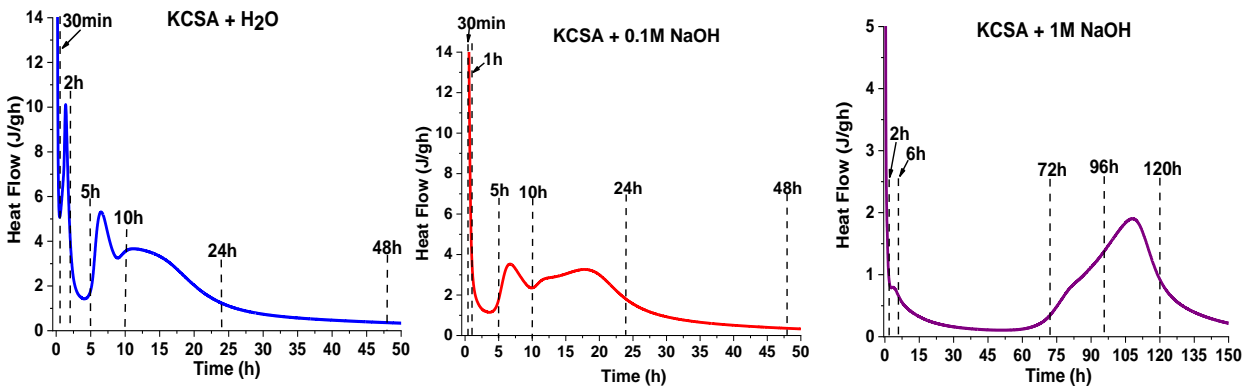


Figure 2. Calorimetric curves for KCSA hydrated with water, 0.1 M or 1 M NaOH

The differences between the reference curve found for the water-hydrated paste and the ones generated by the materials hydrated with NaOH widened with the concentration of the alkali. At 2 M NaOH (KCSA-2M) a 30 min peak preceded a short induction period, followed by the appearance of an intense exothermal peak with two shoulders (Figure 3, left). The first

was recorded at 3 h to 4 h, followed by the main peak at 15 h and the second shoulder after 22 h. The induction period resembled that for the water-hydrated paste and was clearly shorter than observed for KCSA-1M. At 4 M NaOH (KCSA-4M) the induction period was again much longer and signal intensity much lower (Figure 3, centre). That behaviour reversed in the 8 M NaOH (KCSA-8M), with a shorter induction period and the presence of two peaks. The first denoted the beginning of hydration and the second, at 25 h and more intense, the precipitation of hydration products (Figure 3, right).

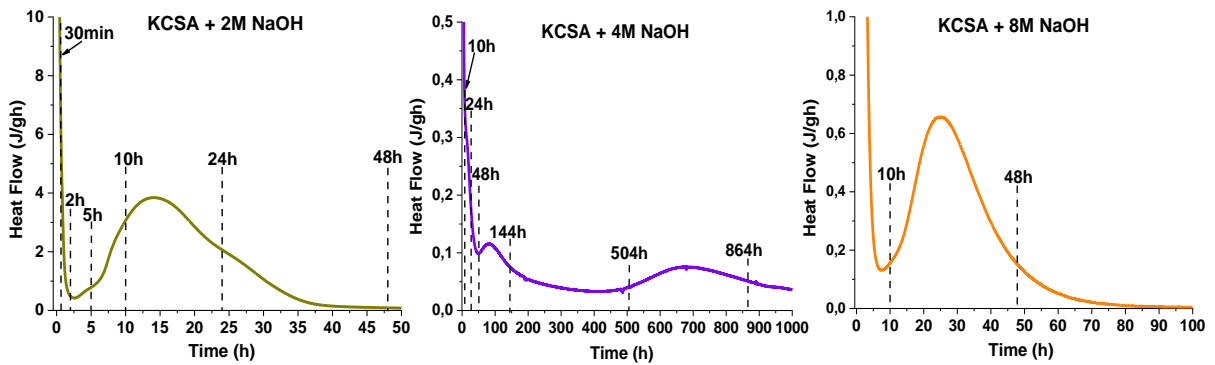


Figure 3. Calorimetric curve for KCSA hydrated with 2 M, 4 M or 8 M NaOH

The findings of the continuous (during hydration) and discontinuous (after detaining the reaction with isopropanol) XRD and FTIR studies conducted at the ages labelled in Figures 2 and 3 to explain the implications of these signals are discussed hereunder.

3.2 Continuous X-ray diffraction

The continuous X-ray diffractograms (30 min intervals over 25 h on hydrating pastes) for the water- and (0.1 M, 1 M, 2 M, 4M and 8 M) NaOH-hydrated clinker are reproduced in Figure 4.

The ye'elimite signal declined quickly and the ettringite diffraction line rose visibly on the pattern for the water-hydrated paste. The KCSA pastes hydrated with 0.1 M to 8 M NaOH generated more amorphous diffractograms than KCSA-H. The presence of alkalis was observed to retard ettringite formation at lower (≤ 2 M) and inhibit it altogether at higher (4 M and 8 M) concentrations, where ettringite instability resulted in the formation of other phases [1-2,14,15,22,23].

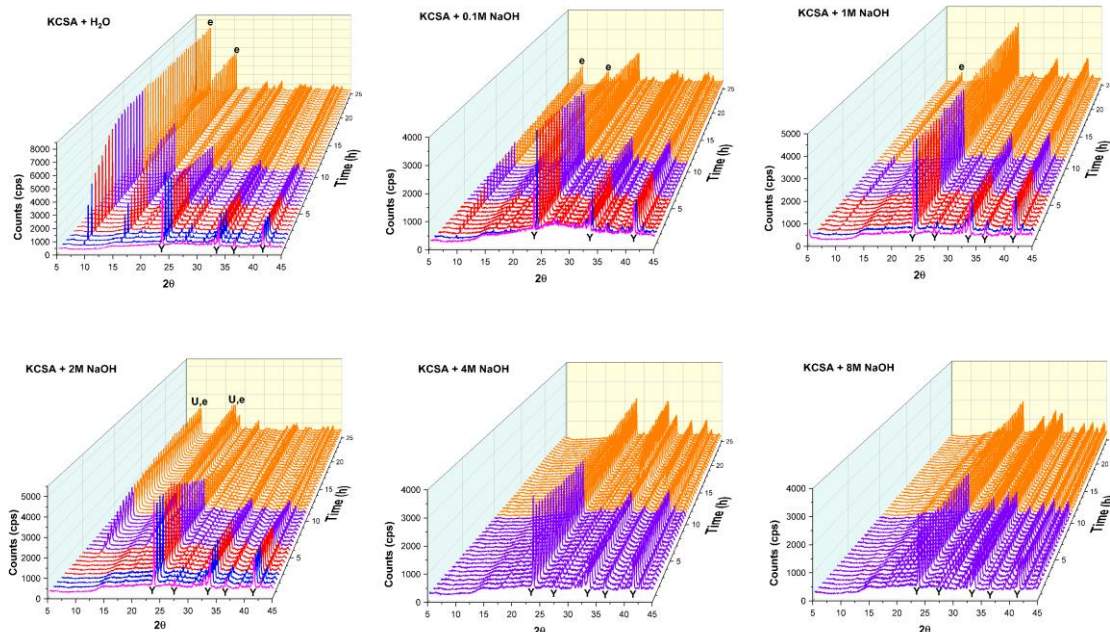


Figure 4. Continuous XRD for water- and NaOH-hydrated clinker (legend: e = ettringite; U = U-phase)

The continuous XRD patterns for the specific ages selected in Figures 2 and 3, before and after each signal, are reproduced in Figure 5 to more clearly display the variations. The pattern for the starting clinker contained signals for the main mineralogical phases present: ye'elimite, belite and bredigite. The 30 min diffractogram for KCSA-H was very similar to the starting pattern, exhibiting no new crystalline phases. Ettringite was the main phase formed after 2 h, although alumina trihydrate was also observed and the intensity of the signals for both rose with hydration time [23-26].

When the clinker was hydrated with 0.1 M and 1 M NaOH, ettringite also formed as the main hydration product, likewise along with both the gibbsite and bayerite forms of alumina trihydrate (Figure 5). Nonetheless, the **ettringite lines** on these diffractograms were less intense and appeared at later ages than the signals observed on the patterns for the water-hydrated pastes. The ye'elimite signals, in turn, were more intense in the former, suggesting the consumption of less ye'elimite in KCSA-0.1M and especially in KCSA-1M.

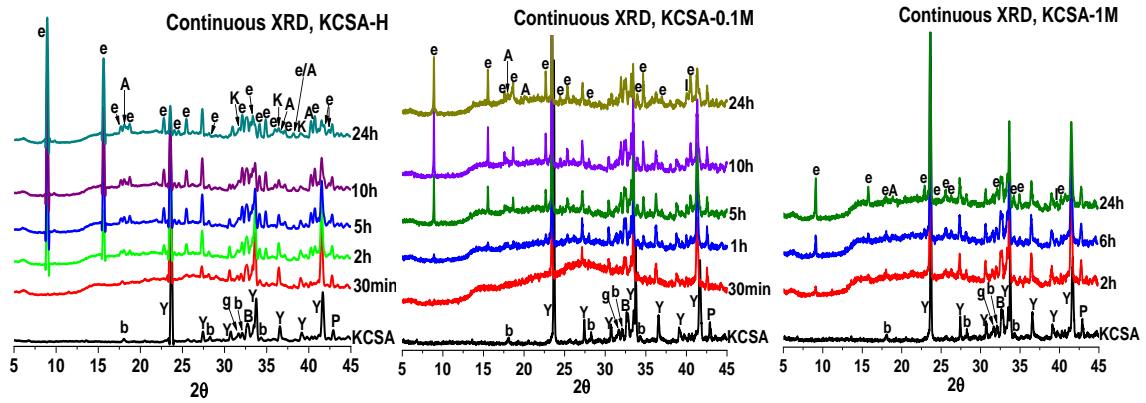


Figure 5. Continuous diffractograms for clinker hydrated with water, 0.1. M or 1 M NaOH at selected ages (legend: e, ettringite; A, alumina trihydrate; k, katoite; Y, ye'elimite; B, bredigite; g, gehlenite; b, belite; P, periclase)

A selection of continuous diffractograms obtained for the pastes hydrated with 2 M, 4 M or 8 M NaOH are reproduced in Figure 6. The <5 h patterns for paste KCSA-2M exhibited signals associated with U-phase [27], which declined with hydration time, giving way to ettringite formation after 10 h.

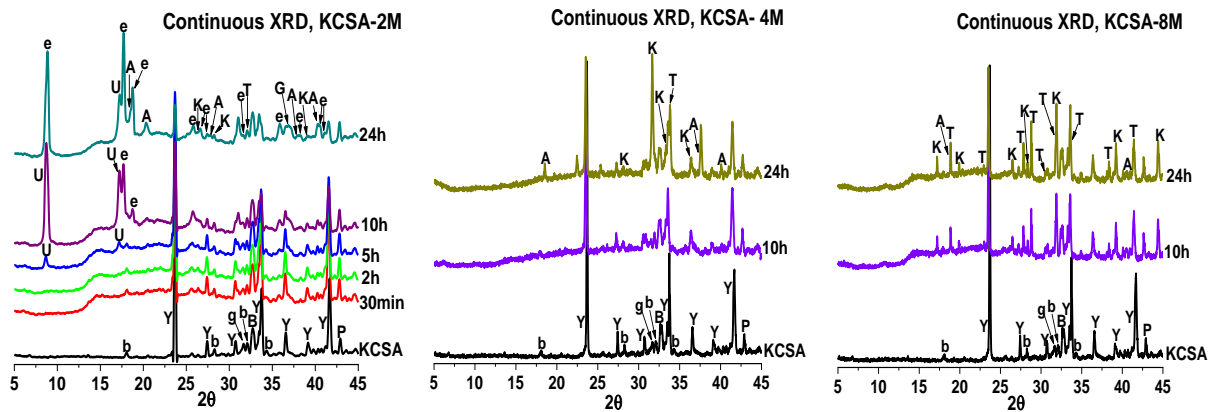


Figure 6. Continuous diffractograms for clinker hydrated with water, 2 M, 4 M or 8 M NaOH at selected ages (legend: e, ettringite; A, alumina trihydrate; U, U-phase; K, katoite; T, thenardite; Y, ye'elimite; B, bredigite; g, gehlenite; b, belite; P, periclase)

The phases forming most abundantly in pastes KCSA-4M and KCSA-8M were thenardite and katoite, along with alumina trihydrate. The respective signals rose with hydration time (Figure 6).

3.3 Post-hydration phase characterisation

The results of XRD and FTIR analysis of the pastes hydrated with water and NaOH at different concentrations upon detention of hydration with isopropanol at the specified times (sub-section 3.2) are set out in this sub-section.

➤ XRD findings

The diffractograms for the powders studied are reproduced in Figure 7. In some cases hydration was allowed to run for 48h, 72 h, 21 d and even 36 d, given that in some samples the heat flow curves peaked at times of over 25 h. The pastes in which hydration was detained were labelled ‘powder’ or ‘discontinuous’ samples to distinguish them from the ones in which the paste was still hydrating.

One of the most prominent differences between the continuous and the discontinuous diffractograms in the first 25 h was the apparently lower degree of phase (especially ettringite) crystallisation in the latter. Authors of earlier studies have reported that same finding [28-29], associated with the combination of a number of factors. i) The continuous XRD radiation targeting the sample in continuous analysis might accelerate the initial reaction. ii) According to the literature, although the method used to detain hydration is the one best suited to samples with AFm-like phases, its possible effect on such phases cannot be ruled out. Scrivener et al. [30] noted that storing samples for up to 24 h in methanol, ethanol or isopropanol dehydrated calcium monosulfoaluminate, which lost two water molecules in the interlayer, simultaneously affected by alcohol seepage. Mantellato et al. [31] noted that the effect of isopropanol-induced detention on ettringite diffraction lines at the time of detention varied depending on the conditions prevailing. iii) Continuous and powder diffraction recording parameters differ slightly.

A comparison of the patterns in Figure 5 to those in Figure 7 for paste KCSA-H revealed that in the continuous diffractograms the intensity of the lines associated with new phase formation was greater or smaller than that of the signals associated with anhydrous phases. The diffractograms for the powder samples exhibited an apparently lower degree of hydration (higher intensity of anhydrous phase lines) than the patterns for the same samples recorded continuously, supporting the hypothesis that the heat generated to obtain

continuous XRD records may accelerate hydration. The same finding was observed in all the other samples (compare Figures 5 and 6 to Figure 8).

As noted, the powder samples were studied at ages of over 25 h. The 48 h and 72 h patterns for pastes KCSA-H exhibited calcium aluminate formation (CAH_{10}) [32]. Similar behaviour was observed in paste KCSA-0.1M, with less intense signals in the powder sample diffractograms and the appearance of lines compatible with CAH_{10} formation in the 48 h and later patterns that intensified with hydration time. The pattern for KCSA-1M also resembled the preceding two, although with no CAH_{10} formation.

The differences between the continuous and discontinuous diffractograms were widest in paste K-2M. No U-phase formation was observed in the powder paste at any age, whereas in the hydrating pastes it was the main phase in the first 10 h. That may have been because U-phase, whilst detected in the latter, is metastable and highly sensitive to variations in pH. The diffractograms for powder samples were also lacking signals denoting the presence of AFt prior to 25 h. After that time low intensity diffraction lines were observed for ettringite, AH_3 , thenardite and katoite, although the width of the signals was indicative of scant crystallinity.

The continuous and discontinuous diffractograms were most similar for pastes KCSA-4M. No signals for AFt were detected, whereas thenardite and katoite were observed at 10 h and the lines for alumina trihydrate after 25 h.

No ettringite [13-15] was observed, in turn, in the discontinuous patterns for KCSA-8M at any of the ages studied. The 10 h XRD patterns for this paste exhibited C_3AH_6 and thenardite as the main crystalline phases, along with alumina trihydrate, whereas in the continuous diffractograms those phases were observed slightly earlier (after 2 h). Another difference was the presence of calcium carboaluminate ($\text{C}_4\text{A}\hat{\text{C}}\text{H}_{11}$) in the powder sample but not in the hydrating paste.

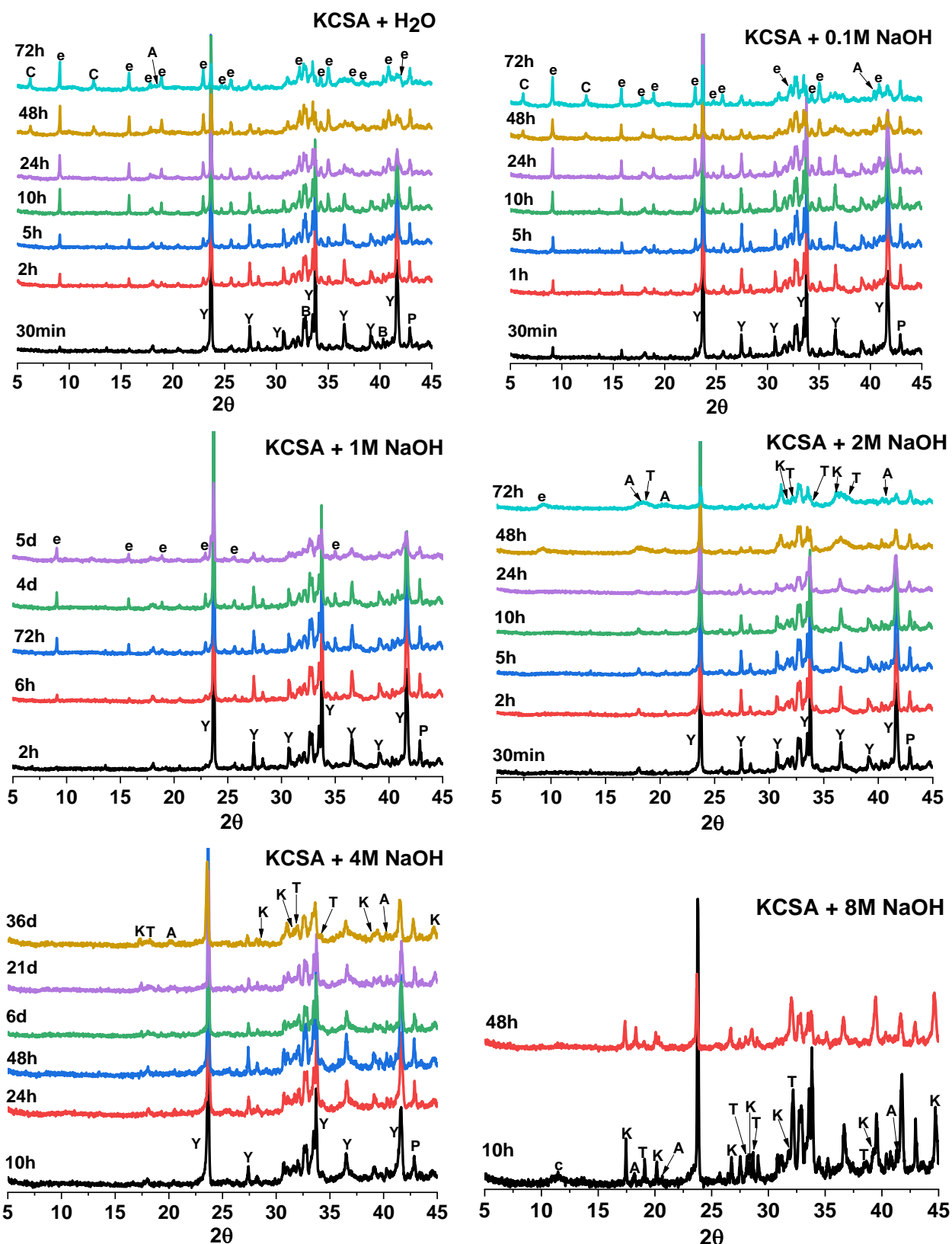
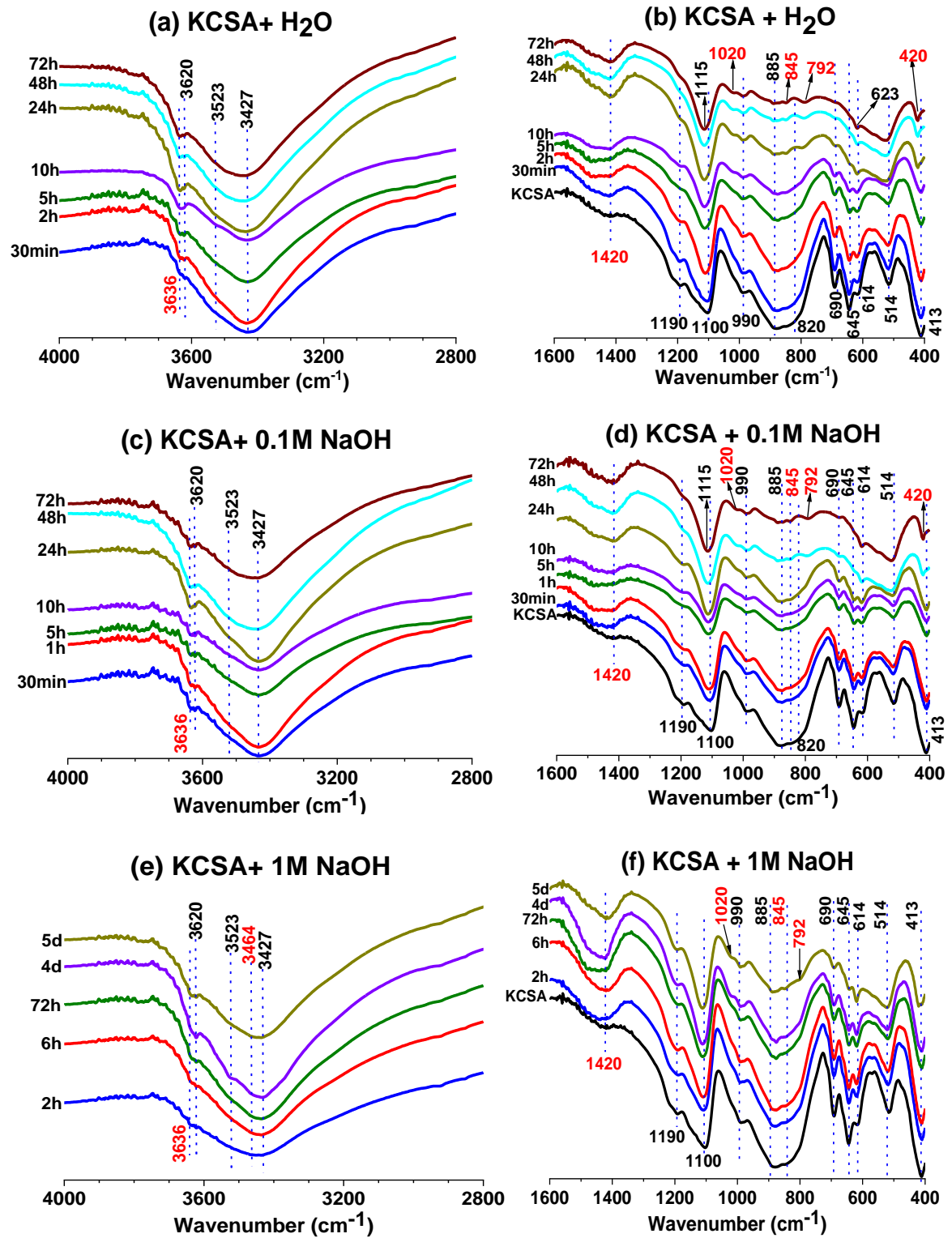


Figure 7. X-ray diffractograms for KCSA clinker hydrated with water, 0.1 M, 1 M, 2 M, 4 M or 8 M NaOH solutions at different ages (legend: Y, ye'elimite; b, belite; B, bredigite; g, gehlenite; P, periclase; C, CAH₁₀; e, ettringite; A, AH₃; T, thenardite; K, katoite; c, C₄A·H₁₁)

➤ FTIR

The FTIR spectra for the powder samples at the ages studied, reproduced in [Figures 8, 9 and 10](#) along with the spectrum for anhydrous KCSA for comparison, confirmed and supplemented the XRD findings. The most prominent bands on the spectrum for anhydrous KCSA were associated with ye'elimite ($C_4A_3\hat{S}$), with vibrations at 1190 cm^{-1} and 1115 cm^{-1} , although vibrations for sulfate groups were also observed (at 1100 cm^{-1} and 614 cm^{-1}), along with those for aluminates, AlO_4 (at 990 cm^{-1} , 885 cm^{-1} , 820 cm^{-1} , 690 cm^{-1} , 645 cm^{-1} and 413 cm^{-1}) [\[33,34\]](#). The presence of C_2S in KCSA was inferred by the bands due to Si-O group vibrations at 990 cm^{-1} , 845 cm^{-1} and 514 cm^{-1} [\[35\]](#). The bands associated with vibrations generated by minority phases overlapped with those described. C_3A , for instance, is known to induce asymmetric vibration bands (AlO_4) at 792 cm^{-1} and two symmetric vibration bands (AlO_4) at 623 cm^{-1} and 413 cm^{-1} [\[36\]](#), although due to dilution and aforementioned overlapping they were difficult to identify.

The spectra for samples KCSA-H, KCSA-0.1M and KCSA-1M ([Figure 8](#)) were very similar. After hydration the ye'elimite bands were observed to decline in intensity or shift slightly, whilst the bands associated with Si-O bonds varied less visibly. The band at 1115 cm^{-1} denoted the presence of ettringite, confirmed by the ones at 990 cm^{-1} , 845 cm^{-1} , 623 cm^{-1} and 420 cm^{-1} and at higher frequencies by weak bands at 3636 cm^{-1} and 3427 cm^{-1} indicative of OH stretching and at 1656 cm^{-1} (band not shown on the figure) of OH bending [\[37\]](#). Overlapping in other bands typical of ettringite made them difficult to distinguish. AH_3 (a phase difficult to detect with XRD given its low crystallinity) was characterised by bands at around 3620 cm^{-1} , 3523 cm^{-1} and 3464 cm^{-1} associated with OH bond stretching vibrations ([Figure 8](#)), at 1020 cm^{-1} associated with Al-OH bending and at 792 cm^{-1} , 623 cm^{-1} , 614 cm^{-1} , 514 cm^{-1} and 420 cm^{-1} with AlO_4 stretching vibrations. The shoulder at 1020 cm^{-1} could also be associated with the presence of CAH_{10} [\[38\]](#), along with the signal at 524 cm^{-1} due to AlO_4 vibration, although given the low intensity and overlapping in those bands they cannot be readily attributed. In addition to the foregoing signals, a number of bands indicative of the CO bond in carbonates (not clearly visible in XRD) were observed, namely at 1420 cm^{-1} and 845 cm^{-1} [\[35-39\]](#). A comparison of the spectra for pastes KCSA-H, KCSA-0.1M and KCSA-1M showed that at the ages studied the most significant changes over time were detected in the water-hydrated paste and the least in the 0.1 M NaOH hydrated cement, indicative of a lower degree of reaction in the latter.



317

318 **Figure 8.** FTIR spectra for KCSA hydrated with: (a)(b) water; (c)(d) 0.1 M NaOH; (e)(f) 1 M NaOH

319

320 The presence of signals for the alumina trihydrates gibbsite (3620 cm^{-1} and 3372 cm^{-1}) and
 321 bayerite (3523 cm^{-1} and 3464 cm^{-1}) prevailed in the spectra for paste KCSA-2M from the

earliest ages (Figure 9). The bands at 3636 cm^{-1} and 3427 cm^{-1} , and at 990 cm^{-1} , 845 cm^{-1} , 623 cm^{-1} and 420 cm^{-1} , were indicative of ettringite formation [37]. The most prominent new band, positioned at 3660 cm^{-1} , along with the (overlapped) band at 990 cm^{-1} and the band at 524 cm^{-1} , was associated with C_3AH_6 formation [38-40] (Figure 9). Thenardite formation, observed with XRD, was also confirmed by the presence of bands at 1100 cm^{-1} and 623 cm^{-1} , associated with SO_4^{2-} bond vibrations. The signal observed at 1020 cm^{-1} might be associated with the presence of AH_3 , whilst the bands at 792 cm^{-1} , 623 cm^{-1} , 614 cm^{-1} , 514 cm^{-1} and 420 cm^{-1} might be due to AlO_4 bonds [36-38]. As in the preceding pastes, the signals observed at 1420 cm^{-1} and 845 cm^{-1} were due to paste carbonation.

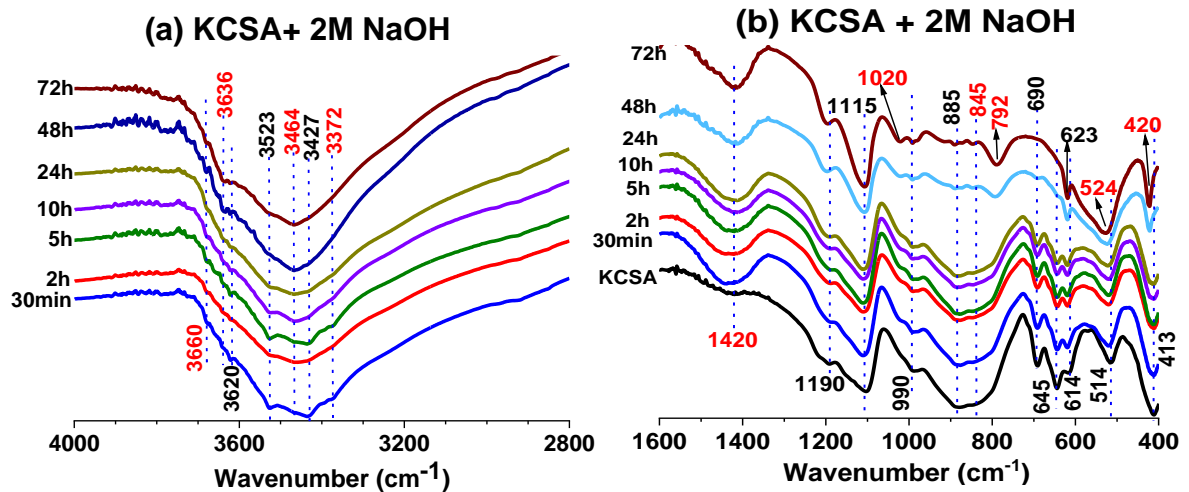


Figure 9. FTIR spectra for KCSA clinker hydrated with 2 M NaOH

A number of signals appeared in the high frequency zones for pastes KCSA-4M and KCSA-8M (Figure 10). Katoite formation was confirmed by the signals at 3660 cm^{-1} and 3545 cm^{-1} whilst the band at 990 cm^{-1} denoted OH bonds and the one at 524 cm^{-1} AlO_4 groups. Thenardite was confirmed by the bands at 1100 cm^{-1} and 623 cm^{-1} . The signals at 3620 cm^{-1} , 3523 cm^{-1} and 3464 cm^{-1} denoted stretching bonds associated with AH_3 formation, likewise indicated by the signals at 1020 cm^{-1} (AlOH bending) and the AlO_4 stretching vibrations at 792 cm^{-1} , 623 cm^{-1} , 614 cm^{-1} , 514 cm^{-1} and 420 cm^{-1} . As in the preceding pastes, bands attributable to CO bonds in carbonates were detected at 1420 cm^{-1} and 845 cm^{-1} [34,36-39].

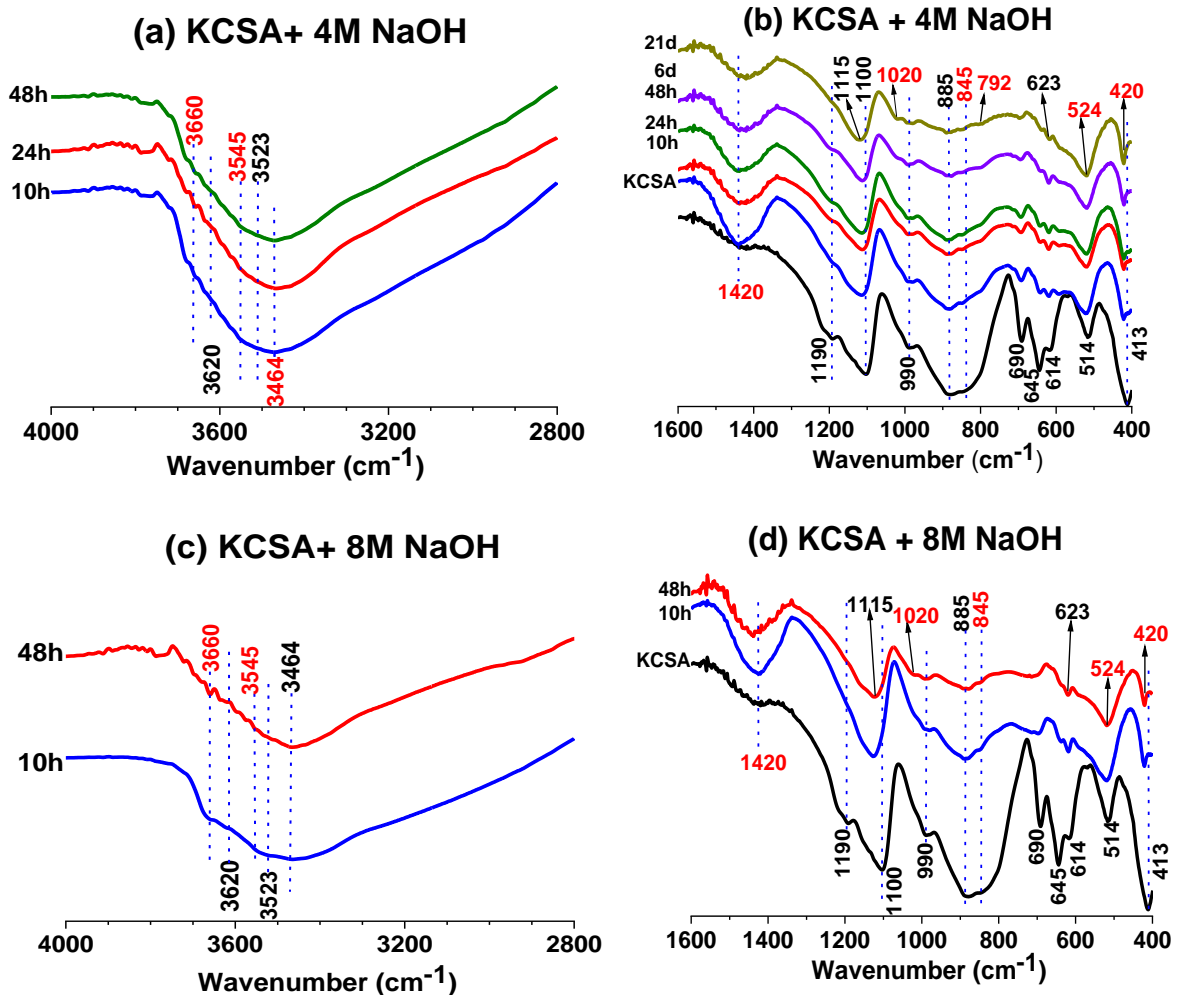


Figure 10. FTIR spectra for CSA cement hydrated with: (a)(b) 4M NaOH; (c)(d) 8M NaOH

4. Discussion

It is known that alkalis can have a significant influence, both favorable and unfavorable, on the properties and performance of PC [41,42] or CSA [13-15] cements. It is important to know this effect well in order to determine the biability of making hybrid alkaline cements using KCSA or CSA, high content of supplementary cementitious materials (ash, slag, puzolans) and an alkaline activator. In previous works, the effect of alkalis at long ages was analyzed in both KCSA [15] and CSA cements [13,14]. The goal of this work is to fill some knowledge gaps, about the effect of alkalis in the early hydration of (KCSA), trying to answer the questions asked by the referees in previous works.

A preliminary study [43] to analyse setting in pastes KCSA-H and KCSA-2M showed that setting times appeared on the heat flow curves in the form of a narrow and intense pre-induction period peak centred at 1.5 h. The inference is that KCSA pastes set as the result of

the formation of a ‘primary ettringite’ prior to material hardening. The present research focused on interpreting how the presence of moderate or high alkali content affected initial hydration kinetics and identifying the early age products forming.

The variation in intensity over time in the main diffraction lines on both the continuous and discontinuous patterns is depicted in Figures 11, 12 and 13. The total heat released is also plotted on the graphs. The most prominent difference between the curves for the hydrating and powder samples was the smaller number of counts observed for all the hydrated phases (ettringite in particular) in the latter after 25 h, as noted in the results.

Early age reactivity in KCSA hydrated with water or solutions with low Na^+ and OH^- concentration (≤ 1 M)

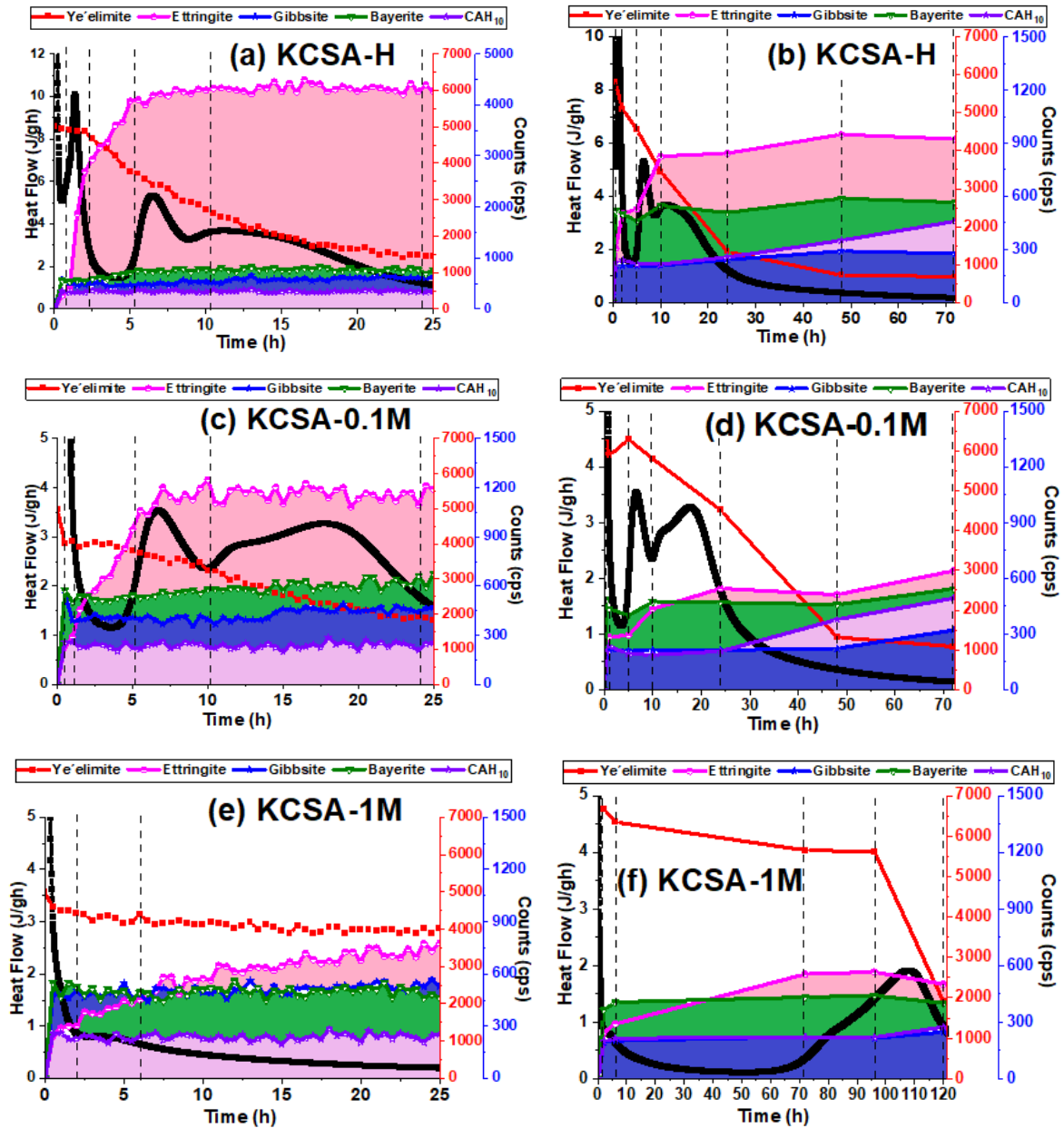
In the water-hydrated clinker (KCSA-H Figure 11(a) and (b)) the calorimetric peak that appeared between 1 h and 2 h was associated with the initial consumption of ye’elimite and the formation of a small amount of the aforementioned primary ettringite [44]. Ye’elimite consumption and ettringite precipitation rose substantially between 2 h and 5 h. Both processes peaked at 5 h to 10 h, as attested to by an intense peak on the calorimetric curve. After 10 h, however, ye’elimite consumption waned whilst ettringite formation tended to flatten. The peak appearing on the heat flow curves was associated in this case with a slight rise in the degree of AH_3 crystallisation as bayerite and gibbsite and the formation of other low crystallinity hydrates such as CAH_{10} . Although no continuous XRD data were collected after 25 h, the XRD analyses for the powder samples (Figure 11(b)) confirmed that ye’elimite consumption had stabilised. After that time the lines associated with ettringite formation and the presence of ye’elimite barely varied, although the intensity of the lines indicative of the presence of AH_3 and CAH_{10} were observed to rise slightly.

As noted earlier, the paste with 0.1 M NaOH (Figure 11(c) and (d)) exhibited behaviour very similar to that observed for the reference. Although more ye’elimite was apparently consumed than in the water-hydrated sample in the first 30 min, the process subsequently slowed and line intensity declined. Those values are consistent with the apparently lower consumption of ye’elimite and amount of ettringite initially formed observed with XRD. The AH_3 forming in the first hour remained unvaried thereafter. As in KCSA-H, in KCSA-0.1M ettringite formation appeared to stabilise after 10 h.

Hydration was found to be retarded in the KCSA-1M pastes (Figure 11(e) and (f)). Both the continuous and discontinuous XRD patterns confirmed nearly nil ye’elimite reactivity in the

first 25 h. Ettringite, AH_3 and to a lesser extent CAH_{10} were observed to grow slightly at 3 h
to 6 h, when a low intensity peak was observed on the heat flow curve. Further to the XRD
findings, the peak appearing at 72 h to 180 h on that curve (as in the preceding pastes) was
associated primarily with Aft and AH_3 formation, confirming the delay in KCSA hydration
reactions in the presence of 1 M NaOH.

398



399

400 **Figure 11.** Comparison of variation in intensity of the most prominent (continuous and
401 discontinuous) diffraction lines to calorimetric curves: (a)(b) KCSA-H; (c)(d) KCSA- 0.1M; (e)(f)
402 KCSA-1M

The FTIR data (Figure 8) confirmed the XRD results for the powder samples. The signals at 3636 cm⁻¹, 3427 cm⁻¹, 1656 cm⁻¹, 1115 cm⁻¹, 990 cm⁻¹, 845 cm⁻¹, 623 cm⁻¹ and 420 cm⁻¹ on the spectra confirmed the presence of ettringite. The ones at 3620 cm⁻¹, 3523 cm⁻¹ and 3464 cm⁻¹, along with the bands at 1020 cm⁻¹, 792 cm⁻¹, 623 cm⁻¹, 614 cm⁻¹, 520 cm⁻¹ and 514 cm⁻¹ confirmed the presence of AH₃. The presence of CAH₁₀ was corroborated by the signals at 1020 cm⁻¹ and 524 cm⁻¹. Although XRD did not detect paste carbonation, the presence of carbonates was confirmed by the signals at 1420 cm⁻¹ and 845 cm⁻¹ on the FTIR spectra.

In summary, the behaviour observed for pastes with alkalinity of 1 M or lower (KCSA-0.1M and KCSA-1M) was similar to the findings for the water-hydrated material (KCSA-H). The major phases observed were AFt, AH₃ (gibbsite, bayerite) and somewhat later CAH₁₀. The presence of alkalis at low concentrations retarded phase formation, possibly because pH affects ettringite stability with a decline in its formation and precipitation rates, favouring early age AH₃ formation. As observed in Figure 1, however, the heat of hydration was similar in the three pastes.

Early age reactivity in KCSA hydrated with a solution containing 2 M NaOH

Process kinetics proceeded more rapidly in the KCSA-2M than in the KCSA-1M pastes (Figure 12). The XRD findings showed greater ye'elimite consumption from the outset, similar to the rates observed for pastes KCSA-H and KCSA-0.1M, although the reaction products differed in paste KCSA-2M, which exhibited the widest differences between the continuous and discontinuous XRD patterns. The continuous diffractogram showed a metastable phase (U-phase) not detected in the powder samples. U-phase (4CaO·0.9Al₂O₃·1.1SO₃·0.5Na₂O·16H₂O), a metastable calcium sulfoaluminate hydrate containing Na⁺ ions in its structure, has a morphology reminiscent of calcium monosulfoaluminate [14,22,27]. It forms in the presence of SO₄²⁻ and Na⁺ ions in high pH media and converts to ettringite when medium alkalinity declines. Its formation, which here occurred primarily in the first 7 h, appeared as the first shoulder on the calorimetric curves (Figure 12 (a)). The intense 10 h peak on the heat flow curve was associated with the higher intensity of the lines indicative of U-phase formation and the steady rise in the amount of ettringite present. After that time the amount of U-phase tended to decline, with ettringite

becoming the predominant phase. The total heat released at that same time also rose substantially (Figure 1). When KCSA was hydrated with 2M NaOH (pH>14), the high alkalinity prevented ettringite precipitation. Na⁺ ion fixation in the form of U-phase or thenardite and the decline in OH⁻ ions as a result of initial alumina trihydrate precipitation may have subsequently lowered the medium pH to values accommodating ettringite precipitation.

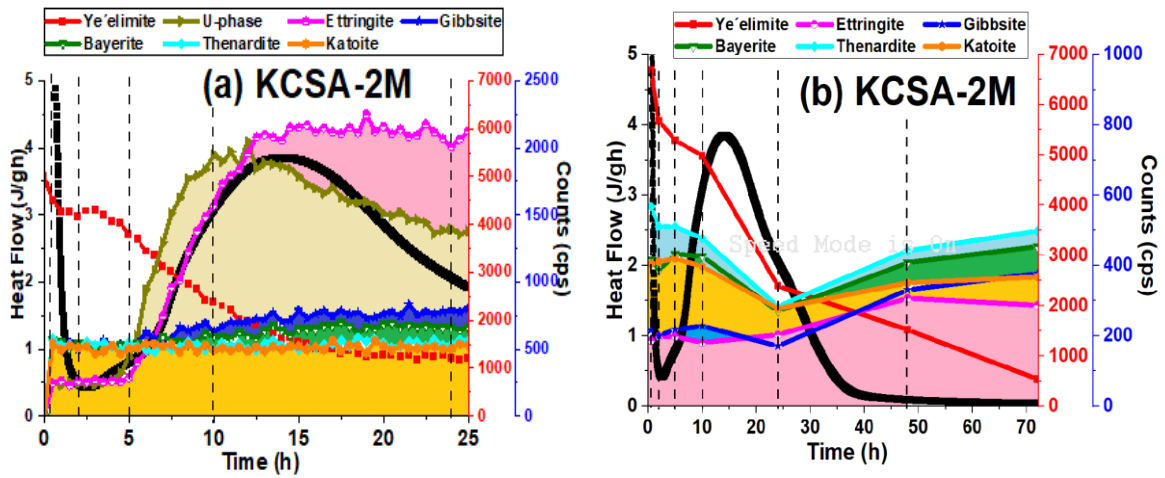
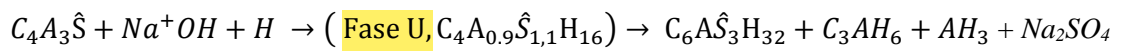


Figure 12. Comparison of variation in intensity of the most prominent continuous (a) and discontinuous (b) diffraction lines to calorimetric curves for KCSA-2M.

As noted earlier, the presence of this phase was the primary difference between the continuous and discontinuous XRD patterns. When paste hydration was detained with isopropanol only ettringite was detected. The present authors believe that finding may be related to AFt and AFm phase stability in isopropanol [30,31].

Other phases detected in NaOH-2M included AH₃, thenardite and katoite. Their presence was greater in the powder (where no U-phase was detected) than in the hydrating samples. At the ages of over 25 h behaviour was similar to that observed for KCSA-H. Total heat tended to remain steady (Figure 1), whilst XRD patterns exhibited a rise in phase crystallinity.

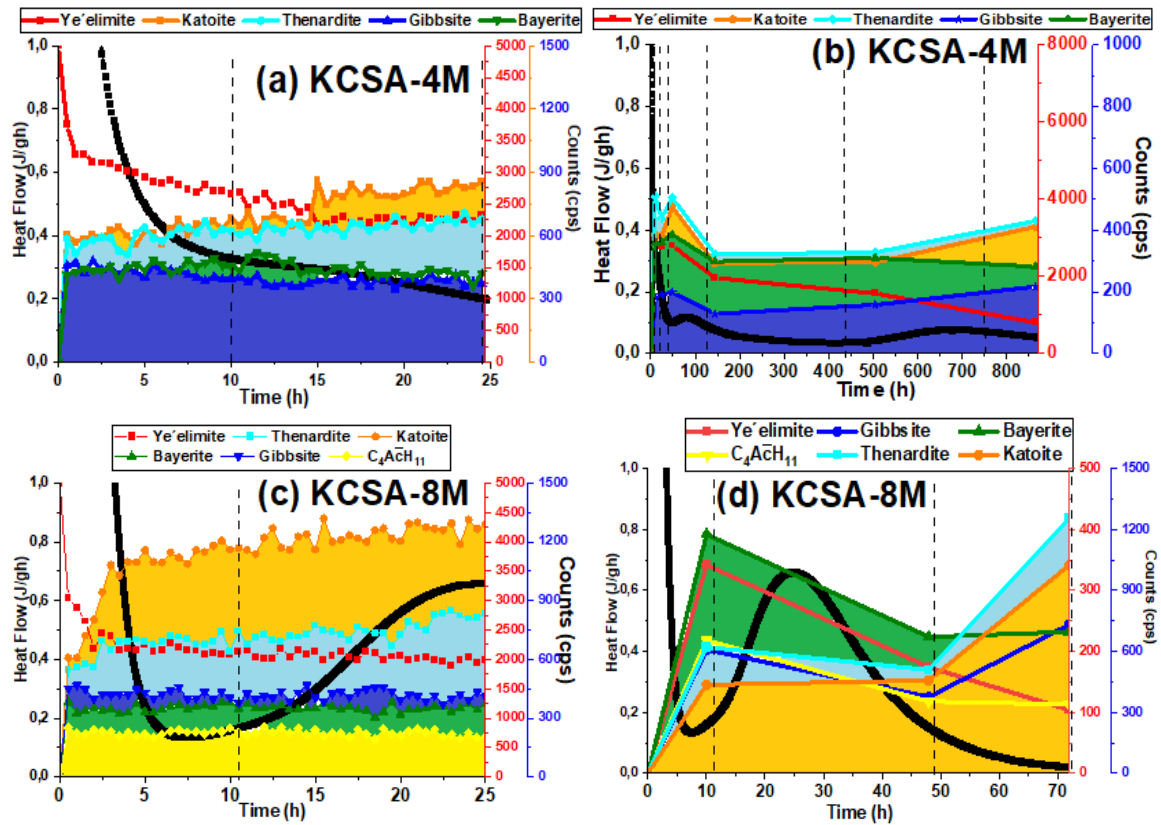
Although the overlapping FTIR signals (Figure 9) were difficult to identify, the bands clearly observed in positions at around 3636 cm⁻¹, 3427 cm⁻¹, 3620 cm⁻¹, 3523 cm⁻¹, 3464 cm⁻¹, 3372 cm⁻¹ and 3660 cm⁻¹ were associated with the presence of ettringite, AH₃ and katoite [30,31]. Thenardite was further confirmed by the signals at 1100 cm⁻¹ and 623 cm⁻¹. As noted earlier, U-phase formation was not detected with either discontinuous XRD or FTIR. Consequently the KCSA-2M system exhibited the formation of metastable phases that evolved to more stable phases such as ettringite, alumina trihydrate and small amounts of thenardite and katoite, further to an initial reaction that might be as follows:



Early age reactivity in KCSA hydrated with solutions containing high Na⁺ and OH-concentrations (4 M or 8 M)

The hydration rates observed in pastes KCSA-4M and KCSA-8M exhibited divergent patterns. In the 4 M paste, the main heat flow peak (Figure 3) was delayed to times of over 25 h, an effect similar to that observed for paste KCSA-1M. In both pastes (KCSA-4M and KCSA-8M), however, the initial ye'elimite content was observed to decline steeply in the first 1 h or 2 h, with a tendency to stabilise or decrease more slowly. Another significant finding was the absence of ettringite or U-phase formation in these high alkalinity pastes (Figure 13). Katoite, thenardite and AH₃ were clearly detected in paste KCSA-4M after 15 h, whereas in paste KCSA-8M katoite and thenardite were present after 2 h, the former apparently more abundantly.

Hydration with a 4 M solution induced ye'elimite decline after 48 h, the same time as hydration products were observed to form and the first calorimetric peak to appear. The second peak, observed after 500 h, was associated with katoite and thenardite formation. At the higher concentration (8 M NaOH), ye'elimite declined and katoite and thenardite formed rapidly. Those hydration products appeared at the same time as the hydration peak on the calorimetric curve. The energy required for these compounds was less than needed to form ettringite [45] ($\Delta_f H^\circ$ (ettringite) = -17 535.00 kJ/mol; $\Delta_f H^\circ$ (C₃AH₆) = -5537.30 kJ/mol, $\Delta_f H^\circ$ (thenardite) = - 1387.00 kJ/mol). That would partially explain the lower heat released (Figure 1) despite the high degree of ye'elimite reaction.



489

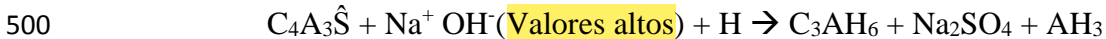
490

491 **Figure 13.** Comparison of variation in intensity of the most prominent (continuous and
 492 discontinuous) diffraction lines to calorimetric curves: (a)(b) KCSA-4M; (c)(d) KCSA- 8M.

493

494

495 The FTIR data (Figure 10) confirmed katoite (3660 cm^{-1} , 3545 cm^{-1} , 990 cm^{-1} and 524 cm^{-1})
 496 and thenardite (1100 cm^{-1} and 623 cm^{-1}) formation as the main reaction products in both
 497 pastes, along with signals indicative of AH_3 and the presence of calcium carboaluminate.
 498 XRD (Figure 7), however, failed to detect the latter in paste KCSA-4M. The respective
 499 reaction might be as follows:



501

502

503

5 Conclusions

This article describes a study of early age reactivity in calcium sulfoaluminate clinker hydration with liquids containing different concentrations of alkalis. The findings showed that including NaOH may retard or accelerate hydration depending on the concentration, which has a significant effect on the type of hydration product formed.

The calorimetric curves for the systems KCSA-H, KCSA-0.1M and KCSA-1M were fairly similar, although the peaks were delayed and declined in intensity with rising NaOH concentration. The values reached when total heat plateaued were likewise similar, as were the hydration products. The delay was associated primarily with the lower stability of AFt formation due to the possibly higher pH in the 1 M NaOH solution.

A faster hydration rate was observed in KCSA-2M than in the 1 M paste, although the total heat was lower in the former than in the reference, KCSA-0.1M and KCSA-1M. That behaviour was associated with the formation of different reaction products. The higher concentration of alkalis favoured (metastable) U-phase formation, a product that converted to AFt at the same time as other phases such as alumina trihydrate, C_3AH_6 and thenardite precipitated.

Hydration with very alkaline (4M and 8M) solutions inhibited AFt formation completely, although ye'elimite reacted more vigorously with rising concentrations (particularly with 8 M NaOH) to form katoite, AH_3 and thenardite. The presence of calcium carboaluminate (C_4AcH_{11}) was also detected in these pastes.

The XRD findings, whether continuous or discontinuous (in pastes with isopropanol-detained hydration), identified the same mineral phases, although minor differences were observed in signal intensity. Those discrepancies might be related to different degrees of phase crystallinity induced by the heat generated in continuous XRD. The most prominent difference, however, was the detection of a metastable phase (U-phase) with the continuous but not the discontinuous methodology.

Acknowledgments

Funding for this study was provided by the Spanish Ministry of Science, Innovation and Universities and ERDF under project BIA2016-76466-R and grant BES-2017-082022. PhD.

student Pilar Padilla-Encinas benefited from the support of the Autonomous University of Madrid to perform the research for her thesis through the IETcc's Applied Chemistry Programme. The cement supplied by HeidelbergCement Hispania is gratefully acknowledged.

Author Contributions

Conceptualisation; methodology, formal analysis, A.F-J y P.P-E; writing—original draft preparation P.P-E; validation, investigation, supervision and writing—review and editing all authors. All authors have read and agreed to the published version of the manuscript.

Conflicts of Interest: the authors declare no conflicts of interest.

References

- [1]. N. Fukuda, On the Constitution of Sulfo-Aluminous Clinker, Bull. Chem. Soc. Jpn. 34 (1961) 138–139. <https://doi.org/10.1246/bcsj.34.138>.
- [2]. F. Winnefeld, B. Lothenbach, Hydration of calcium sulfoaluminate cements — Experimental findings and thermodynamic modelling, Cem. Concr. Res. 40 (2010) 1239–1247.
- [3]. M.A.G Aranda, A.G. De la Torre, *Eco- Efficient Concrete*; Elsevier: Amsterdam, The Netherlands, (2013); ISBN 9780857094247.
- [4]. F.P. Glasser, L. Zhang, High-performance cement matrices based on calcium sulfoaluminate–belite compositions, Cem. Concr. Res. 31 (2001) 1881–1886.
- [5]. G Álvarez-Pinazo, I Santacruz, MAG Aranda, AG De la Torre, Advances in Cement Research 28 (2016) (8), 529-543
- [6]. J.H .Sharp, C.D. Lawrence, R. Yang, Calcium sulfoaluminate cements—low- energy cements, special cements or what? Adv. Cem. Res. 11, (1999), 3–13, doi:10.1680/adcr.1999.11.1.3.
- [7]. T. Hanein, J.Galvez- martos, M.N. Bannerman, Carbon footprint of calcium sulfoaluminate clinker production. *J. Clean. Prod.* 2018, 172, 2278–2287, doi:10.1016/j.jclepro.2017.11.183.
- [8]. A.Telesca M. Marroccoli M.L. Pace M. Tomasulo G.L. Valenti P.J.M. Monteiro A hydration study of various calcium sulfoaluminate cements, Cement and Concrete Composites, 53 (2014) 224-232
- [9]. A. Klein, G.E. Troxell, Studies of calcium sulfoaluminate admixtures for expansive cements. ASTM Proc 1958;58:988–1008.
- [10]. J. Zhang, G. Ke, Y. Liu, Early Hydration Heat of Calcium Sulfoaluminate Cement with Influences of Supplementary Cementitious Materials and Water to Binder Ratio. Materials 14, (2021), 642. <https://doi.org/10.3390/ma14030642>
- [11]. P. Chaunsali, P. Mondal, Influence of Calcium Sulfoaluminate (CSA) Cement Content on Expansion and Hydration Behavior of Various Ordinary Portland Cement- CSA Blends, J. Am. Ceram. Soc. 98 (2015) 2617–2624. <https://doi.org/10.1111/jace.13645> .

- [12]. K. Ogawa, D.M. Roy, C_4A_3S hydration, ettringite formation, and its expansion mechanism III. Effect of CaO, NaOH and NaCl. Conclusions, *Cem. Concr. Res.* 12 (1982) 247–256.
- [13]. Y. Zhang, J. Chang, Microstructural evolution of alumina trihydrate gel during the hydration of calcium sulfoaluminate under different alkali concentrations, *Constr. Build. Mater.* 180 (2018) 655–664.
- [14]. L.U.D. Tambara, M. Cheriaf, J.C. Rocha, A. Palomo, A. Fernández-Jiménez, Effect of alkalis content on calcium sulfoaluminate (CSA) cement hydration, *Cem. Concr. Res.* 128 (2020) 105953.
- [15]. P. Padilla-Encinas, A. Palomo, M.T. Blanco-Varela, A. Fernández-Jiménez, Calcium sulfoaluminate clinker hydration at different alkali concentrations, *Cem. Concr. Res.* 138 (2020) 106251.
- [16]. M. García- Maté, A.G. De La Torre, L. León- Reina, M.A.G. Aranda, I. Santacruz, Hydration studies of calcium sulfoaluminate cements blended with fly ash. *Cem. Concr. Res.*, 54, (2013), 12–20, doi:10.1016/j.cemconres.2013.07.010.
- [17]. S. Joseph; R. Snellings, Ö. Cizer, Activation of Portland cement blended with high volume of fly ash using Na_2SO_4 . *Cem. Concr. Compos.* 104, (2019), 103417, doi:10.1016/j.cemconcomp.2019.103417.
- [18]. S. Donatello, A. Fernández- Jimenez, A. Palomo, Very high volume fly ash cements. Early age hydration study using Na_2SO_4 as an activator. *J. Am. Ceram. Soc.* 96, (2013), 900–906, doi:10.1111/jace.12178.
- [19]. I. García- Lodeiro, A. Fernández- Jiménez, A. Palomo, Variation in hybrid cements over time. Alkaline activation of fly ash Portland cement blends. *Cem. Concr. Res.* 52, (2013), 112–122, doi:10.1016/j.cemconres.2013.03.022.
- [20]. S. Alahrache, F. Winnefeld, J.B. Champenois, F. Hesselbarth, B. Lothenbach, Chemical activation of hybrid binders based on siliceous fly ash and Portland cement, *Cem. Concr. Compos.* 66 (2016) 10–23, <https://doi.org/10.1016/j.cemconcomp.2015.11.003>.
- [21]. Q. Xu, J. Hu, J.M.J. Mauricio Ruiz, K.Wang, Z. Ge, Isothermal calorimetry tests and modeling of cement hydration parameters, *Thermochimica Acta* 499 (2010) 91–99.
- [22]. M.J. Sánchez-Herrero, A. Palomo, A. Fernández-Jiménez, $C_4A_3\check{S}$ hydration in different alkaline media, *Cem. Concr. Res.* 46 (2013) 41–49.
- [23]. M. Ben Haha, F. Winnefeld, A. Pisch, Advances in understanding ye’elimite-rich cements, *Cem. Concr. Res.* 123 (2019) 105778. <https://doi.org/10.1016/j.cemconres.2019.105778>.
- [24]. C.J. Hampsoim, J.E. Bailey, On the structure of some precipitated calcium aluminosulphate hydrates, *J. Mater. Sci.* 17 (1982) 3341–3346. <https://doi.org/10.1007/BF01203504>.
- [25]. F.P. Glasser, Thermodynamic investigation of the $CaO-Al_2O_3-CaSO_4-H_2O$, 22 (n.d.) 13.
- [26]. F. Goetz-Neunhoeffler, J. Neubauer, P. Schwesig, Mineralogical characteristics of Ettringites synthesized from solutions and suspensions, *Cem. Concr. Res.* 36 (2006) 65–70. <https://doi.org/10.1016/j.cemconres.2004.04.037>.
- [27]. G. Li, P.L. Bescop, M. Moranville, The U-phase formation in cement-based systems containing high amounts of Na_2SO_4 , *Cem. Concr. Res.* 26 (1996) 27–33.
- [28]. D. Jansen, J.J. Wolf, N. Fobbe, The hydration of nearly pure ye’elimite with a sulfate carrier in a stoichiometric ettringite binder system. Implications for the hydration process based on in-situ XRD, 1H-TD-NMR, pore solution analysis, and thermodynamic modeling, *Cem. Concr. Res.* 127 (2020) 105923. <https://doi.org/10.1016/j.cemconres.2019.105923>.

- 627 [29]. M. Montes, E. Pato, P.M. Carmona-Quiroga, M.T. Blanco-Varela, Can
628 calciumaluminates activate ternesite hydration?, *Cem. Concr. Res.* 103 (2018) 204–
629 215. <https://doi.org/10.1016/j.cemconres.2017.10.017>
- 630 [30]. K. Scrivener, R. Snellings, B. Lothenbach, eds., *A Practical Guide to Microstructural*
631 *Analysis of Cementitious Materials*, 0 ed., CRC Press, 2018.
632 <https://doi.org/10.1201/b19074>.
- 633 [31]. S. Mantellato, M. Palacios, R.J. Flatt, Impact of sample preparation on the specific
634 surface area of synthetic ettringite, *Cem. Concr. Res.* 86 (2016) 20–28.
635 <https://doi.org/10.1016/j.cemconres.2016.04.005>.
- 636 [32]. F. Bullerjahn, E. Boehm-Courjault, M. Zajac, M. Ben Haha, K. Scrivener, Hydration
637 reactions and stages of clinker composed mainly of stoichiometric ye'elimite, *Cem.*
638 *Concr. Res.* 116 (2019) 120–133.
- 639 [33]. N.J. Calos, C.H.L. Kennard, A.K. Whittaker, R.L. Davis, Structure of Calcium
640 Aluminate Sulfate C_4A_3S , *J. Solid State Chem.* 119 (1995) 1–7.
- 641 [34]. M.J.S. Herrero, La activación alcalina como procedimiento para el desarrollo de
642 nuevos cementos belíticos, Tesis Dr. Univ. Nac. Educ. Distancia. (2017) 376.
- 643 [35]. N. V. Chukanov, Infrared spectra of mineral species, 2014.
644 <https://doi.org/10.1007/978-94-007-7128-4>.
- 645 [36]. T. Vázquez-Moreno, M.T. Blanco-Varela, Tabla de frecuencias y espectros de
646 absorción infrarroja de compuestos relacionados con la química del cemento, *Mater.*
647 *Constr.* 31 (1981) 31–48. <https://doi.org/10.3989/mc.1981.v31.i182.1007>.
- 648 [37]. S.C.B. Myneni, S.J. Traina, G.A. Waychunas, T.J. Logan, Vibrational spectroscopy
649 of functional group chemistry and arsenate coordination in ettringite, *Geochim.*
650 *Cosmochim. Acta.* 62 (1998) 3499–3514. [https://doi.org/10.1016/S0016-](https://doi.org/10.1016/S0016-7037(98)00221-X)
651 [7037\(98\)00221-X](https://doi.org/10.1016/S0016-7037(98)00221-X).
- 652 [38]. L. Fernández-Carrasco, Aplicación de la espectroscopia infrarroja al estudio de
653 cemento aluminoso, *Mater. Constr.* 46 (1996). DOI:
654 <https://doi.org/10.3989/mc.1996.v46.i241.540>
- 655 [39]. L. Fernández-Carrasco, Carbonatación de pastas de cemento de aluminato de calcio,
656 *Mater. Constr.* 51(263-264): (2001). 127-136, DOI:[10.3989/mc.2001.v51.i263-](https://doi.org/10.3989/mc.2001.v51.i263-264.358)
657 [264.358](https://doi.org/10.3989/mc.2001.v51.i263-264.358)
- 658 [40]. M.A. Trezza, A.E. Lavat, Analysis of the system $3CaO \cdot Al_2O_3 - CaSO_4 \cdot 2H_2O - CaCO_3 -$
659 H_2O by FT-IR spectroscopy, *Cem. Concr. Res.* 31 (2001) 869–872.
- 660 [41]. S.J. Way, A. Shayan, Early hydration of a portland cement in water and sodium
661 hydroxide solutions: Composition of solutions and nature of solid phases, *Cem.*
662 *Concr. Res.* 19 (1989) 759–769. [https://doi.org/10.1016/0008-8846\(89\)90046-X](https://doi.org/10.1016/0008-8846(89)90046-X).
- 663 [42]. H. Ye, A. Radlińska, Effect of Alkalis on Cementitious Materials: Understanding the
664 Relationship between Composition, Structure, and Volume Change Mechanism, *J.*
665 *Adv. Concr. Technol.* 15 (2017) 165–177. <https://doi.org/10.3151/jact.15.165>.
- 666 [43]. P. Padilla-Encinas, A. Palomo, M.T. Blanco-Varela, L. Fernández-Carrasco, A.
667 Fernández-Jiménez, Monitoring early hydration of calcium sulfoaluminate clinker,
668 *Constr. Build. Mater.* 295 (2021) 123578.
669 <https://doi.org/10.1016/j.conbuildmat.2021.123578>.
- 670 [44]. L. Zhang, F.P. Glasser, Hydration of calcium sulfoaluminate cement at less than 24
671 h, *Adv. Cem. Res.* 14 (2002) 141–155.
- 672 [45]. Lothenbach B., Kulik D.A., Matschei T., Balonis M., Baquerizo L., Dilnesa B.,
673 Miron G.D., Myers R.J., , *Cemdata18: A chemical thermodynamic database for*
674 *hydrated Portland cements and alkali-activated materials. Cement and Concrete*
675 *Research* 115 (2019) 472–506

Supplementary information

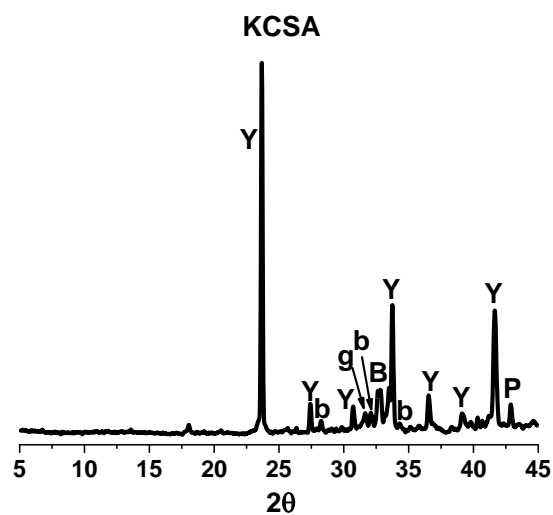


Figure S1. X-ray diffractogram for anhydrous KCSA clinker

